Realization of the Quantum Toffoli Gate with Trapped Ions

T. Monz,[1] K. Kim,[1,*] W. Hänsel,[1] M. Riebe,[1] A. S. Villar,[1,2,†] P. Schindler,[1] M. Chwalla,[1] M. Hennrich,[1] and R. Blatt[1,2]

[1]*Institut für Experimentalphysik, Universität Innsbruck, Technikerstrasse 25, A-6020 Innsbruck, Austria*

[2]*Institut für Quantenoptik und Quanteninformation, Österreichische Akademie der Wissenschaften, Otto-Hittmair-Platz 1, A-6020 Innsbruck, Austria*

(Received 14 November 2008; published 28 January 2009)

Gates acting on more than two qubits are appealing as they can substitute complex sequences of two-qubit gates, thus promising faster execution and higher fidelity. One important multiqubit operation is the quantum Toffoli gate that performs a controlled NOT operation on a target qubit depending on the state of two control qubits. Here we present the first experimental realization of the quantum Toffoli gate in an ion trap quantum computer, achieving a mean gate fidelity of 71(3)%. Our implementation is particularly efficient as the relevant logic information is directly encoded in the motion of the ion string.

DOI: 10.1103/PhysRevLett.102.040501 PACS numbers: 03.67.Lx, 32.80.Qk, 37.10.Ty

The demonstration of a universal set of quantum operations consisting of single- and two-qubit gates marks a milestone towards the realization of a quantum computer. Such operations have been realized with several physical systems [1,2], including nuclear magnetic resonance (NMR), single photons, superconducting devices, cavity QED, and ion traps. A universal operation set allows for implementation of arbitrary algorithms by decomposing the respective unitary operation into sequences of quantum gates. However, this approach scales unfavorably with the complexity of implemented algorithms if only single- and two-qubit gates are available. It makes the demonstration of most algorithms still impossible in current implementations. Gates acting on more than two qubits could significantly simplify the decomposition of otherwise intractable algorithms. Moreover, they promise faster execution and higher fidelity. So far, all demonstrated and fully characterized quantum gates are two-qubit entangling operations, apart from one implementation of a three-qubit Toffoli gate in NMR [3].

The quantum Toffoli gate is probably the archetype of a three-qubit gate. It performs a controlled NOT operation on a target qubit depending on the state of two control qubits. It is valuable in complex quantum algorithms like Shor's algorithm [4] and has immediate practical applications as correcting operation in quantum error correction [3,5]. It constitutes one of the basic building blocks for quantum computation.

For ion traps several schemes for implementing a quantum Toffoli gate have been proposed [6,7]. Here we report on the first experimental realization of the Toffoli gate with an ion trap quantum computer. It requires half the resources compared to schemes based on concatenated two-qubit gates [8]. This significant contraction is achieved by encoding the combined information of the two control qubits in the common vibrational mode of the ion string. A major new aspect of the current work is that higher levels of the vibrational mode are used to temporarily store the combined quantum information of both control qubits during encoding. It shows that quantum computation which exploits the available Hilbert space could allow for a significant speedup of quantum operations in various implementations.

Our experimental system consists of a string of $^{40}Ca^{+}$ ions confined in a linear Paul trap. Each ion represents a qubit, where quantum information is stored in superpositions of the $S_{1/2}(m = -1/2) = |S\rangle \equiv |1\rangle$ ground state and the metastable $D_{5/2}(m = -1/2) = |D\rangle \equiv |0\rangle$ state of the $^{40}Ca^{+}$ ions [9]. The center-of-mass (COM) vibrational mode of the ion string is used to mediate the interaction between the ion qubits. Each experiment includes: (a) the initialization of the qubits and the COM mode in a well-defined state, (b) the actual gate operation and (c) a quantum state measurement. Initialization of the COM mode to the ground state is achieved by Doppler cooling on the $S_{1/2} \leftrightarrow P_{1/2}$ dipole transition followed by sideband cooling on the qubit transition. Optical pumping ensures that all qubits are prepared in $S_{1/2}(m = -1/2)$. The gate operation consists of a series of laser pulses which are applied to individually addressed ions. The electronic and vibrational state of the ion string are manipulated by setting frequency, length, intensity, and phase of the pulses. Single qubit operations are implemented by laser pulses at frequency ω_0 resonant with the transition $|S, n\rangle \leftrightarrow |D, n\rangle$, where n is the phonon number of the state. The motion of the ion string is manipulated by laser pulses at frequency $\omega_0 + \omega_z$, where ω_z is the COM mode frequency along the trap axis ($\omega_z/2\pi \approx 1.2$ MHz), inducing transitions of the kind $|S, n\rangle \leftrightarrow |D, n + 1\rangle$. This allows us to remove a phonon from the system, provided an ion is in the $|D\rangle$ state. Note that the Rabi frequency on this transition is $\Omega_n = \Omega_0\sqrt{n + 1}$. The final state of the ion qubits is measured by scattering light at 397 nm on the $S_{1/2} \leftrightarrow P_{1/2}$ transition and detecting the fluorescence with a CCD camera. The presence or absence of fluorescence of an ion corresponds to a projective measurement in the $\{|S\rangle, |D\rangle\}$ basis. Further

details about the experimental setup can be found in Ref. [9].

The pulse sequence for our implementation of the quantum Toffoli gate consists of three major parts: (i) Encoding of the joint quantum information of the control qubits $|c_1\rangle$ and $|c_2\rangle$ in the vibrational COM mode, (ii) a NOT operation on the target qubit controlled by the vibrational mode, and (iii) the reversal of the encoding step (i). Here, the encoding is the crucial part of the gate. We exploit the fact that it is always possible to add more phonons to the vibrational mode, while phonons can only be subtracted until the vibrational ground state is reached. The joint encoding of the logic control information (c_1 AND c_2) into the vibrational mode can be depicted as a two-step process: Initially, the vibrational mode contains no phonons, i.e. $|\mathrm{vib}\rangle = |n = 0\rangle$. In the first step (first two pulses of the encoding sequence, also see Table I), two phonons are deposited in the COM mode if both control ions are in $|c_1c_2\rangle = |SS\rangle$ while less than two phonons are generated for the other three basis states:

$$
\begin{aligned}
&|c_1c_2, 0\rangle = |SS, 0\rangle \rightarrow |DD, 2\rangle,\\
&|c_1c_2, 0\rangle = |DS, 0\rangle \rightarrow \sin\frac{\pi}{2\sqrt{2}}|DD, 1\rangle + \cos\frac{\pi}{2\sqrt{2}}|DS, 0\rangle,\\
&|c_1c_2, 0\rangle = |SD, 0\rangle \rightarrow \cos\frac{\pi}{2\sqrt{2}}|DD, 1\rangle - \sin\frac{\pi}{2\sqrt{2}}|DS, 0\rangle,\\
&|c_1c_2, 0\rangle = |DD, 0\rangle \rightarrow |DD, 0\rangle.
\end{aligned}
$$

After the first two pulses of the first step, one phonon is removed such that only for the initial state $|c_1c_2\rangle = |SS\rangle$ one phonon remains in the COM mode: After the first two pulses, the first control bit is always in state $|D\rangle$. It allows for removing of one phonon by transferring control ion 1 from $|D, n + 1\rangle$ to $|S, n\rangle$. This is not directly possible in all four cases due to the different coupling strengths on the $|D, 2\rangle \leftrightarrow |S, 1\rangle$ and $|D, 1\rangle \leftrightarrow |S, 0\rangle$ transitions. However, a sequence of pulses of different length and phase can be tailored such that in spite of the different coupling strengths the operation $|D, n + 1\rangle \leftrightarrow |S, n\rangle$ for $n = 0,1$ is realized. The mechanism of this composite pulse sequence—pulses 3–5 in Table I—can be understood using the Bloch sphere picture with state $|D, n + 1\rangle$ as the north pole and $|S, n\rangle$ as the south pole (e.g., see Ref. [9]). Starting from $|D, 2\rangle$, pulse 3 flips the state vector from the north pole to the equator, pulse 4 rotates the vector around itself, and pulse 5 continues the flip to the south pole reaching $|S, 1\rangle$. On the other hand, for the initial state $|D, 1\rangle$, pulse 3 rotates the state vector only partially towards the equator, pulse 4 mirrors the state vector on the equatorial plane, so that pulse 5 can complete the rotation to the south pole $|S, 0\rangle$. For zero phonons nothing changes and thus conserves $|D, 0\rangle$.

Thus, we encode the logic information (c_1 AND c_2) in the vibrational mode as (c_1 AND c_2) $= 1 \Rightarrow |n = 1\rangle$ and (c_1 AND c_2) $= 0 \Rightarrow |n = 0\rangle$. The next part of the Toffoli gate consists of a NOT operation on the target qubit depending on the binary information encoded in the vibrational state. This operation is provided by the Cirac-Zoller controlled NOT gate [10] as demonstrated in [11,12]. Finally, the third part reverses the encoding and restores the vibrational mode to the ground state.

The ideal unitary map implemented by our pulse sequence, see Table I, is given by

TABLE I. Pulse sequence of the Toffoli gate implementation: Laser pulses on the ith ion on the $|S, n\rangle \leftrightarrow |D, n\rangle$ transition are denoted by $R_i(\theta, \phi)$, on the $|S, n\rangle \leftrightarrow |D, n + 1\rangle$ transition by $R_i^+(\theta, \phi)$, with laser phase ϕ and pulse area $\theta = \Omega t$ in terms of Rabi frequency Ω, and pulse length t. For details see Ref. [9]. The gate is completed after $\tau_{\mathrm{gate}} = 1.39$ ms.

#	Pulse	Task	
1	$R_1^+(\pi, \frac{3\pi}{2})$	Map control$_1$ on motion	Encoding $\tau_{\mathrm{encode}} = 512\ \mu$s
2	$R_2^+(\frac{\pi}{\sqrt{2}}, \frac{3\pi}{2})$	Map control$_2$ on motion	
3	$R_1^+(\frac{\pi}{2\sqrt{2}}, \frac{\pi}{2})$	Remove phonon	
4	$R_1^+(\pi, 0)$		
5	$R_1^+(\frac{\pi}{2\sqrt{2}}, \frac{\pi}{2})$		
6	$R_3(\frac{\pi}{2}, 0)$	Prepare target for CNOT	controlled NOT $\tau_{\mathrm{CNOT}} = 362\ \mu$s
7	$R_3^+(\frac{\pi}{2}, 1)$	Composite phase gate	
8	$R_3^+(\sqrt{2}\pi, \frac{\pi}{2})$		
9	$R_3^+(\frac{\pi}{2}, 0)$		
10	$R_3(\frac{\pi}{2}, (\frac{1}{\sqrt{2}} - 1)\pi)$	Finalize CNOT	
11	$R_1^+(\frac{\pi}{2\sqrt{2}}, (-\frac{1}{2} + \frac{1}{\sqrt{2}})\pi)$	Undo encoding	Decoding $\tau_{\mathrm{decode}} = 512\ \mu$s
12	$R_1^+(\pi, (-1 + \frac{1}{\sqrt{2}})\pi)$		
13	$R_1^+(\frac{\pi}{2\sqrt{2}}, (-\frac{1}{2} + \frac{1}{\sqrt{2}})\pi)$		
14	$R_2^+(\frac{\pi}{\sqrt{2}}, (\frac{1}{2} + \frac{1}{\sqrt{2}})\pi)$		
15	$R_1^+(\pi, (\frac{1}{2} + \frac{1}{\sqrt{2}})\pi)$		

$$U_T = \exp\left(-i\pi\frac{1}{2\sqrt{2}}\sigma_{Z,t}\right)\begin{pmatrix}1&0&0&0&0&0&0&0\\0&1&0&0&0&0&0&0\\0&0&1&0&0&0&0&0\\0&0&0&1&0&0&0&0\\0&0&0&0&1&0&0&0\\0&0&0&0&0&1&0&0\\0&0&0&0&0&0&0&i\\0&0&0&0&0&0&-i&0\end{pmatrix}$$

in the basis

$$\{|c_1, c_2, t\rangle\} = \{|DDD\rangle, |DDS\rangle, |DSD\rangle, |DSS\rangle, |SDD\rangle, |SDS\rangle, |SSD\rangle, |SSS\rangle\}.$$

The factor $\exp(-i\pi\frac{1}{2\sqrt{2}}\sigma_{Z,t})$, with the Pauli operator σ_Z, is a phase shift on the target qubit $|t\rangle$. This phase factor can either be included in a redefinition of the computational basis or compensated for by single qubit operations. In total, this unitary evolution is fully equivalent to an ideal Toffoli gate.

The unitary map U_T describes an operation which applies a NOT operation on the target ion if and only if the control ions are in the state $|SS\rangle$. We verify this behavior by preparing the system in all eight basis states and subsequently measuring the output state probabilities after the Toffoli operation. Figure 1 shows a bar graph of these probabilities, the so-called truth table. Ideally, this shows the absolute values of the respective elements of the unitary matrix. On average we obtain probabilities of ≈81% that the ions end up in the correct output state. However, this analysis only reveals the classical features of the gate. Only a more thorough analysis allows us to prove that the desired operation is indeed performed.

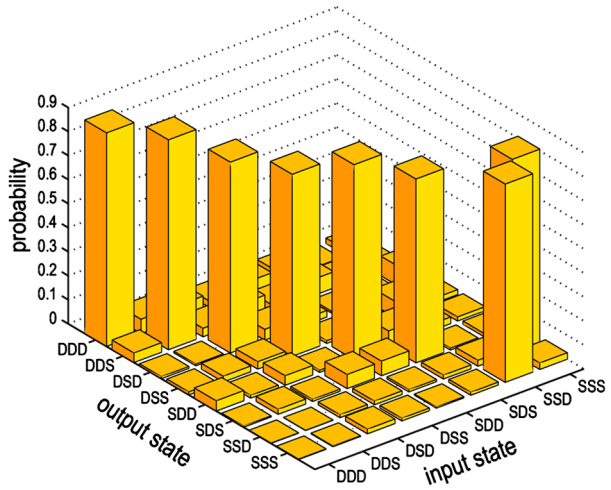

FIG. 1 (color online). Experimentally obtained truth table of the Toffoli gate: After preparing the three ions in one of the eight basis input states $|SSS\rangle$ to $|DDD\rangle$ (right axis) the probabilities of all basis output states (left axis) are measured 100 times. On average the correct output state is reached with a probability of 81(±5)%. The stated error in the measurements is mainly caused by quantum projection noise.

A complete characterization of the action of our pulse sequence must take into account experimental imperfections, in particular, the coupling of our qubits to their environment, which will in general lead to a nonunitary time evolution. Such a characterization is provided by the operator sum representation in which a process $\mathcal{E}$ is described by $\rho_{\text{out}} = \mathcal{E}(\rho_{\text{in}}) = \sum_{m,n=1}^{4^N} \chi_{m,n} A_m \rho_{\text{in}} A_n^\dagger$, where ρ_{in} and ρ_{out} are the input and output density matrices, N is the number of qubits, and A is a basis of operators in the Hilbert space of dimension $2^N \times 2^N$ [13]. The process matrix χ contains all information about the investigated quantum operation and is obtained by quantum process tomography [12,14]. The complete χ-matrix has been obtained experimentally. For visual comparison, absolute values of both the ideal and realized χ-matrices are depicted in Fig. 2. The "fingerprint" of the ideal χ-matrix is clearly visible in the experimental data. A quantitative measure for the performance of the gate operation is the mean gate fidelity $F_{\text{mean}} = \text{mean}_{\psi_i}[\langle\psi_i|U_T^\dagger \mathcal{E}(|\psi_i\rangle \times \langle\psi_i|)U_T|\psi_i\rangle]$, where U_T is the ideal unitary map and the ψ_i are a set of 2×10^5 pure input states randomly drawn according to the Haar measure from the unitary group $U(8)$ [15]. The mean fidelity is the average value of the fidelity between the output state expected from the ideal unitary transformation and the output state calculated from the experimentally determined χ-matrix. For the results shown in Fig. 2, we obtain $F_{\text{mean}} = 71(3)\%$, where the error is due to statistical uncertainties in the tomographic measurements [16]. The observed infidelity is mainly caused by technical imperfections: Addressing errors due to the finite width of the focused laser beam result in a weak excitation of the neighboring ions. For the given setup, the addressing error described by the ratio of the Rabi frequencies of a neighboring, nonaddressed ion to the addressed ion was on the order of 7%, causing an infidelity of ≈12%. Temperature changes and voltage fluctuations of the trap electrodes result in a drift of the vibrational mode frequency. Assuming a detuning from the sideband of 100 Hz, an infidelity of 7% is calculated. Note that these two errors are purely technical imperfections. Remaining infidelity contributions are initialization of the COM mode in the ground state ≈1%, laser linewidth and magnetic field fluctuations ≈1%, and ion state initialization ≈0.5% per ion. The decoherence time of quantum information stored in the vibrational COM mode is on the order of 85 ms, which is consistent with a heating rate on the order of 1 phonon per 140 ms. These two effects do not limit the quantum Toffoli gate at the current stage.

A comparison of this result with the fidelity expected from a realization based on two-qubit CNOT gates highlights the benefits of our scheme. With our experimental setup two-qubit CNOT gates have been demonstrated [12] with a mean fidelity of $F_{\text{mean}} = 92.6\%$. We estimate that a realization of a composite quantum Toffoli gate with six such CNOT gates [14] would result in a gate fidelity of approximately $F = (92.6\%)^6 \approx 63\%$. We note that this is

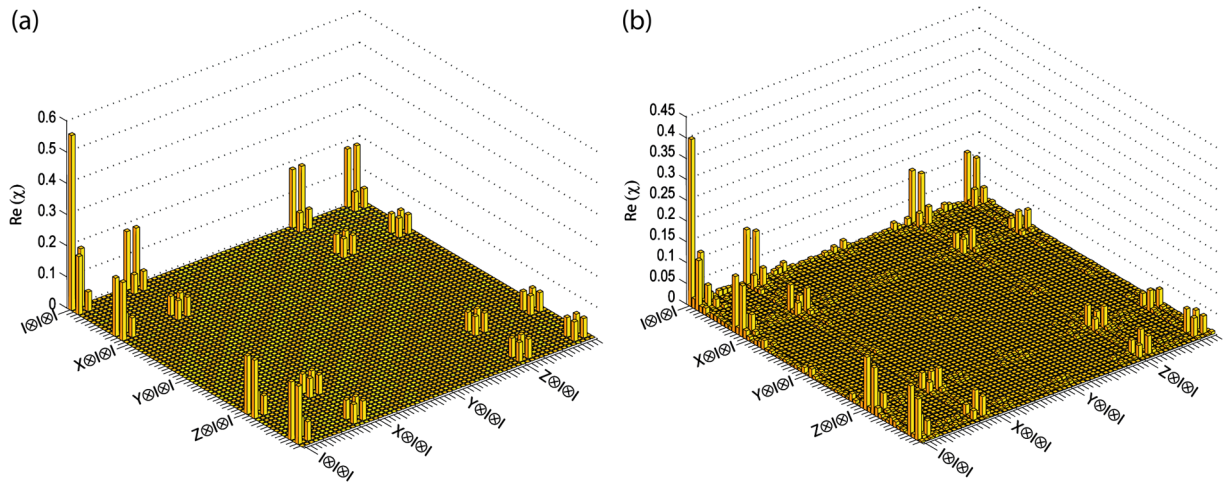

FIG. 2 (color online). Comparison between (a) ideal and (b) experimental process χ-matrices of the Toffoli gate. The absolute values of the elements are shown in the operator basis $\sigma_{c1} \otimes \sigma_{c2} \otimes \sigma_t \in \{I \otimes I \otimes I, I \otimes I \otimes X, \ldots, Z \otimes Z \otimes Z\}$. Ideal and experimental process matrix show a chi overlap $\mathrm{Tr}(\chi_{\mathrm{ideal}}\chi_{\mathrm{exp}}) = 66.6(4)\%$.

an optimistic estimate as it relies on two-ion data only. The duration of our gate is 1.5 ms, which is mainly determined by the coupling strength for transitions of the kind $|S, n\rangle \leftrightarrow |D, n+1\rangle$. A two-qubit controlled NOT gate takes approximately 700 μs [12]. Therefore, realizing a Toffoli gate based on six CNOT gates would be about 3 times longer than the sequence described above. Finally, an adaption of the Toffoli gate proposal using qudits [7] would also be shorter than a decomposition into CNOT gates, but still 30% longer than our sequence.

To conclude, we have shown the first implementation of a three-qubit Toffoli gate with trapped ions. The operation is fully characterized by the first realization of a process tomography on a three-qubit gate. The achieved fidelity of $F_{\mathrm{mean}} = 71(3)\%$ is mainly limited by technical imperfections with room for improvements. Our scheme is notably faster than any other proposed scheme. This particular efficiency is achieved by encoding the relevant logic information of the control qubits in higher phonon states of the vibrational mode. Such encoding may also help to simplify other complex quantum operations and map be applied to any system in which qubits are coupled via a harmonic oscillator. In addition, the Toffoli gate has an immediate practical application in quantum error correction. Here, depending on the state of the qubits carrying the error syndrome a conditional bit flip has to be applied to the qubits carrying the information [3,5]. This task can either be accomplished by a projective measurement followed by classically controlled operations or directly by the Toffoli gate. The latter approach is particularly favorable in quantum systems where a projective measurement is not feasible or not efficient.

During preparation of this manuscript we became aware of a similar realization of a quantum Toffoli gate with a photonic system, reported in [17].

We gratefully acknowledge support by the Austrian Science Fund (FWF), by the European Commission (SCALA, CONQUEST networks), and by the Institut für Quanteninformation GmbH. This material is based upon work supported in part by IARPA.

*Present address: Department of Physics and Joint Quantum Institute, University of Maryland, College Park, MD, 20742, USA.

†Present address: Institute of Optics, Information and Photonics, Max Planck Research Group, University of Erlangen-Nuernberg, Staudtstrasse 7/B2, 91058 Erlangen, Germany.

[1] Karen Southwell, Quantum Coherence (Nature Insight), Nature (London) **453**, 1003 (2008).
[2] P. Zoller *et al.*, Eur. Phys. J. D **36**, 203 (2005).
[3] D. G. Cory *et al.*, Phys. Rev. Lett. **81**, 2152 (1998).
[4] L. M. K. Vandersypen *et al.*, Nature (London) **414**, 883 (2001).
[5] M. Sarovar and G. J. Milburn, Proc. SPIE Int. Soc. Opt. Eng. **5842**, 158 (2005).
[6] C.-Y. Chen and S.-H. Li, Eur. Phys. J. D **41**, 557 (2007).
[7] T. C. Ralph, K. J. Resch, and A. Gilchrist, Phys. Rev. A **75**, 022313 (2007).
[8] D. Maslov and G. Dueck, Electron. Lett. **39**, 1790 (2003).
[9] F. Schmidt-Kaler *et al.*, Appl. Phys. B **77**, 789 (2003).
[10] J. I. Cirac and P. Zoller, Phys. Rev. Lett. **74**, 4091 (1995).
[11] F. Schmidt-Kaler *et al.*, Nature (London) **422**, 408 (2003).
[12] M. Riebe *et al.*, Phys. Rev. Lett. **97**, 220407 (2006).
[13] I. L. Chuang and M. A. Nielsen, J. Mod. Opt. **44**, 2455 (1997).
[14] M. A. Nielsen and I. L. Chuang, *Quantum Computation and Quantum Information* (Cambridge University Press, Cambridge, England, 2000).
[15] M. Pozniak, K. Zyczkowski, and M. Kus, J. Phys. A **31**, 1059 (1998).
[16] C. F. Roos *et al.*, Phys. Rev. Lett. **92**, 220402 (2004).
[17] B. P. Lanyon *et al.*, Nature Phys., advanced online publication: 2008/12/07, (2008), http://dx.doi.org/10.1038/nphys1150.